Shot noise and higher current moments in dimensions 2, 3 & 4

I. Travěnec
Institute of Physics, Slovak Academy of Sciences, Dúbravská cesta 9, 84511 Bratislava, Slovakia

February 2, 2008

Abstract

Shot noise and higher current moments $T_M = \langle \mathrm{Tr}(t^\dagger t)^M \rangle$ are studied within the Anderson model of disordered conductors in dimensions $d = 2, 3$ and 4. Here t denotes a transmission matrix. We calculate the conductance $G = T_1$, shot noise $S = T_1 - T_2$, Fano factor $F = S/G$ and ratios $C_M = T_M/G$, and we show indications that all of them are as good order parameters as the conductance itself. In the limit of infinite system size, two limiting values of F and C_M are found; the stable one in the metallic regime, and the unstable one, characterizing the critical point for $d > 2$. We present analytical expressions for both limiting values, together with a compact formula for current cumulants at 3D criticality. Our data confirm also Nazarov's microscopic theory [PRB **52**, 4720 (1995)], as we show numerically for special linear combinations of T_M.

1 Introduction

Much effort has been devoted to the Anderson localization [1]. The transport in disordered systems exhibits many universal features, like universal conductance fluctuations (UCF) in the metallic regime, or $\ln G$ - type distribution in the insulator.

Theoretical approach concentrated mainly, but not exclusively, on one-dimensional (1D) models. The type of scaling of the conductance distribution was investigated in 1D [2] and numerically in 3D [3]. Muttalib et al. [4] analyzed and generalized the DMPK equation also beyond quasi-1D and calculated the distribution function of G in all regimes. They tried to apply the generalized DMPK also to localized states [5]; in the metallic case it was applied successfully before [6]. Beenakker and Büttiker [7] also studied the metallic transport in dimension $d > 1$ and we will utilize their results for all current moments.

Besides the UCF, i. e. the second cumulant of G (or *var* G), numerous other exact quantitities where proposed in the metallic regime (see this Intro and Section 2), but only few in the other regimes. The main purpose of this work is to calculate a complete set of quantities at 3D metal-insulator transition (MIT) exactly. It contributes to theoretical description of the criticality from different side than microscopic theory, RMT, non-linear σ-model, DMPK, etc.

Besides the Landauer's conductivity $G = \mathrm{Tr}\ \mathcal{T}$ (in units $2e^2/h$), and shot noise power $S = \mathrm{Tr}[\mathcal{T} - \mathcal{T}^2]$, where $\mathcal{T} = t^\dagger t$, also the universal properties of higher order current moments in terms of $\mathcal{T}^M$ were observed [8]. The third current cumulant was given analytically also in the limit of frequency and temperature both zero:

$$\langle\langle I^3\rangle\rangle \ = \langle I^3\rangle - 3\langle I^2\rangle\langle I\rangle + 2\langle I\rangle^3 = \langle I\rangle \ \frac{\langle \mathrm{Tr}[\mathcal{T}(1-\mathcal{T})(1-2\mathcal{T})]\rangle}{\langle \mathrm{Tr}\ \mathcal{T}\rangle} = \frac{\langle I\rangle}{15} \qquad (1)$$

$\langle ...\rangle$ means ensemble averaging. This formula holds for large systems in diffusive (metallic) regime and we will reproduce it later.

Let us denote the higher current moments $T_M = \langle \mathrm{Tr}\ [\mathcal{T}^M]\rangle$. These quantities were analyzed in the works [9] and [10]. The exact solution for normalized moments on 1D Anderson chain

$$C_M = \frac{T_M}{T_1} = \frac{\Gamma(M-\frac{1}{2})^2}{\Gamma(M)^2\Gamma(\frac{1}{2})^2} \qquad (2)$$

was confirmed by numerical simulations. This formula applies exclusively to pure 1D. Analogical exact expressions for higher dimensions were given in [7] for the metallic transport, Eqs. (22) or (8), and we will add those for 3D critical regime.

Let us make a note on relationship of cumulants and moments. Compact expressions for charge (i. e. also current) cumulants $\ll Q^k \gg$ in diffusive regime were derived in [11]. These cumulants can be calculated with help of a characteristic function

$$\ln \chi(u) = \sum_{k=1}^{\infty} \frac{u^k}{k!} \ll Q^k \gg \qquad (3)$$

where χ is Fourier transformed probability distribution of charges. Assuming mutual independence of channels they found

$$\ll Q^k \gg \propto \sum_j \Big(\mathcal{T}(1-\mathcal{T})\frac{d}{d\mathcal{T}}\Big)^{k-1}\mathcal{T}\big|_{\mathcal{T}=\mathcal{T}_j} \qquad (4)$$

where the sum over eigenvalues means trace. We get shot noise as the second cumulant, proper part of Eq. (1) as the third one, etc. Thus the current cumulants and moments are connected in a different way than e. g. those ones of conductivity.

The moments T_M themselves become usually either zero (insulator) or infinite (metal) in the large system limit, except criticality. But we will show, that both their ratios and appropriately chosen linear combinations will have non-trivial finite values. The limiting C_M ratios have the pleasant property that they are independent of boundary conditions.

The shot noise $S = T_1 - T_2$ and Fano factor $F = 1 - C_2$ of Anderson model have been studied in [12] for dimensions $d = Q1D, 2$ and in [13] for $d = 3$. Q1D means quasi-1D systems, i. e. stripes of fixed, but large enough width and even much larger length. We continue in 2D and 3D with larger systems and statistics, and we add both $d = 4$ and higher current moments $M \geq 3$. Under simple assumptions on the distribution function of Lyapunov exponents, one gets the limiting values for C_M both in diffusive and critical (3D) regimes. We will also confirm the validity of Nazarov's theory [14] in diffusive case for higher moments and in $d = 4$; for $M = 2$ and $d = Q1D, 2, 3$ it was already shown in [12] and [13], though less precisely because of smaller system sizes and thus larger disturbing ballistic effects.

There is a great amount of literature on shot noise, e. g. [7], [8]. The Poissonian value $F \to 1$ corresponds to the strongly localized (insulating) regime, the well known $1/3$ suppression $F = 1/3$ is typical for the metallic regime. If $d > 2$ we get yet another value F_C, which marks the MIT. All higher moments will show qualitatively the same behaviour.

In recent paper [15] even the fourth cumulant, or the combination $C_3 - C_4$ was introduced. Such quantities can be calculated in general.

The aim of this work is to show that C_M and special linear combinations of T_M converge to universal values in the large system size limits; to observe two non-trivial limiting C_M values for $d > 2$; to give them analytically (except 4D criticality) and to prove them numerically.

The paper is organized as follows. In this Intro and in Section 2.1 we recall some results from papers, treating higher current moments or cummulants, especially in metallic regime, and the first steps towards 3D criticality. Then we add theoretical predictions for any normalized moment and cummulant at 3D MIT. In the next Section 2.2 we briefly introduce Nazarov's microscopic model, yielding even more information about the moments in metallic regime. In Section 3 we confirm virtually any given analytical formula for current moments and cummulants by numerical simulations (except 1D and Q1D).

2 Model, Numerical Method and Theory

Let us consider the Anderson model with the Hamiltonian

$$H = \sum_n \epsilon_n |n><n| + \sum_{[nn']} |n><n'| + |n'><n| \tag{5}$$

where the diagonal disorder ϵ_n is taken randomly from $< -W/2, W/2 >$, i.e. it has uniform (box) distribution, and $[n, n']$ are nearest neighbor sites of a d-dimensional cubic lattice. Concerning numerical calculations, the transfer matrix method of the calculation of moments and especially the way how to deal with larger systems was described in [9].

2.1 Limiting values of Fano factor, C_M and current cumulants

Lyapunov exponents λ_n are related to the eigenvalues $\mathcal{T}_n$ of $\mathcal{T}$ as follows:

$$\mathcal{T}_n = \cosh^{-2}(\lambda_n) \tag{6}$$

It has long been known, that the smallest (most important) λ_n exponents are distributed equidistantly in large metallic systems, i. e. that their distribution function $P(\lambda)$ is constant. In the work [7] this was used to calculate general diffusive C_M. Constant density was observed numerically and approved by various analytical treatments. Numerical data, however, indicate that in the critical regime (3D, 4D) $P(\lambda)$ reaches the origine, and it is not constant. To generalize the results, we can propose that at least for small λ, the $P(\lambda) \propto \lambda^\alpha$. We know already that $\alpha = 0$ in metallic regime, irrespective of dimension. Replacing the trace, i. e. summation of eigenvalues, by an integral over $P(\lambda)d\lambda$ - which works for large enough systems - we get:

$$C_M(\alpha) = \frac{\int_0^\infty \lambda^\alpha \cosh^{-2M}(\lambda) d\lambda}{\int_0^\infty \lambda^\alpha \cosh^{-2}(\lambda) d\lambda} \tag{7}$$

Now let us summarize the metallic regime. The one-third-suppression $F = 1 - C_2 = 1/3$ was confirmed in [7]. We can also reproduce the Eq. (1), namely $1 - 3C_2 + 2C_3 = 1/15$. The term proposed in [15] is nothing but the fourth cumulant: $F - 6(C_2 - C_3) + 6(C_3 - C_4) = -1/105$. And generally for the Fano-factor-like quantities we get $C_M - C_{M+1} = C_M/(2M + 1)$, with

$$C_M(0) = \frac{4^{M-1}(M-1)!^2}{(2M-1)!} \tag{8}$$

which is yet another practical form of Eq. (22), [7]. An analogy of Eq. (7) was proposed already in [9], just with unspecified distribution function.

In [16] it was shown that $\alpha = 1$ in 3D at MIT. This was utilized in [13] to calculate the limiting value of Fano factor in the critical regime. We can give this value exactly: $F_C = 1 - C_2(1) = 1/3 + 1/(6 \ln 2)$. In Appendix A the integrals of interest are solved analytically. Useful values of $C_M(\alpha)$ are summarized in Table 1.

The $\alpha = 1$ is correct not only for $P(\lambda)$, but also for the distribution of the first (smallest) Lyapunov exponent $P(\lambda_1)$, even with the same slope. That is

why the fits are perfect for all moments - for numerically treated finite systems the higher moments depend almost exclusivelly on $P(\lambda_1)$. The possibility of $\alpha = 2$ was proposed in [17] for 4D at MIT; we will come to this point later.

Let us return to the current cumulants. The generating function $\ln \chi_\alpha(u)$ from Eq. (3) was calculated for the $\alpha = 0$ case in [11]:

$$\ln \chi_0(u) = Q_0 \int_0^\infty d\lambda \ln\Big(\frac{e^u - 1}{\cosh^2(\lambda)} + 1\Big) = Q_0 \ \mathrm{arcsinh}^2\sqrt{e^u - 1} \tag{9}$$

where the charge Q_0 involves constants and physical units, see [11], and it is non-universal, depending on model parameters like disorder W. Using Eq. (3) they calculated the cumulants $\ll Q \gg /Q_0 = 1$, $\ll Q^2 \gg /Q_0 = 1/3$, $\ll Q^3 \gg /Q_0 = 1/15$, see Eq.(1), $\ll Q^4 \gg /Q_0 = \ll Q^5 \gg /Q_0 = -1/105$, see above, etc. In the case $\alpha = 1$ we get a rather formal formula (Appendix A)

$$\begin{aligned} \ln \chi_1(u) &= Q_0' \int_0^\infty \lambda \ln\Big(\frac{e^u - 1}{\cosh^2(\lambda)} + 1\Big) d\lambda = -2Q_0' \int_0^{t^*} \Big(t \ln 2 - L(t)\Big) dt = \\ &= Q_0' \ln 2 \ \mathrm{arcsinh}^2\sqrt{e^u - 1} + 2Q_0' \int_0^{t^*} L(t) dt \end{aligned} \tag{10}$$

where $t^* = i \ \mathrm{arcsinh}\sqrt{e^u - 1}$ and the Lobachevsky function, see [18]:

$$L(z) = -\int_0^z \ln(\cos(x)) dx = \frac{z^3}{6} + \frac{z^5}{60} + \frac{z^7}{315} + \mathcal{O}(z^9) \tag{11}$$

We can calculate the cumulants at 3D criticality, taking again the derivatives of $\ln \chi_1(u)$ at $u \to 0$:

$$\ll Q \gg = Q_0' \ \ln 2 = T_1 \tag{12}$$

$$\ll Q^2 \gg = Q_0' \ \Big(\frac{1}{3} \ln 2 + \frac{1}{6}\Big) = T_1 - T_2 \tag{13}$$

$$\ll Q^3 \gg = Q_0' \ \Big(\frac{1}{15} \ln 2 + \frac{2}{15}\Big) = T_1 - 3T_2 + 2T_3 \tag{14}$$

$$\ll Q^4 \gg = Q_0' \ \Big(-\frac{1}{105} \ln 2 + \frac{11}{210}\Big) = T_1 - 7T_2 + 12T_3 - 6T_4 \tag{15}$$

We added relations in terms of T_M from Eq. (4). The above-mentioned value $F_C = \ll Q^2 \gg / \ll Q \gg$.

2.2 Diffusive T_M values from Microscopic theory

The diffusive contribution to eigenvalues of $\mathcal{T}$ was calculated in [14]. Nazarov introduced a function $\delta F(\phi)$, and he showed that $P(\lambda)$ is proportional to real part of $\sin\phi \ \delta F(\phi)$ at special complex ϕ and that

$$\delta F(\phi) = \mathrm{Tr}\Big(\frac{\mathcal{T}}{1-\mathcal{T}\sin^2\,\frac{\phi}{2}}\Big) = -\frac{2\phi}{\sin\phi}\sum_s \frac{1}{s^2-\phi^2} \tag{16}$$

Here the Cooperon mode energies $s^2 = \pi^2(n_1^2 + n_2^2 + ... + n_d^2)$, $n_1 = 1, 2, ...$, $n_2 = 0, 1, ...$, ..., $n_d = 0, 1, ...$ for simple d-dimensional cube with hard wall boundary conditions. The index n_1 refers to one chosen transfer direction. The minor changes for samples with periodic boundary conditions were described e. g. in [19]. There is analyzed the 3D case of $G = T_1$, because the sum on the rhs of Eq. (16) diverges for $d \geq 2$ and a cut-off on wave vectors' length is useful. Some other details can be found in [20]. ϕ is the global phase shift between left and right side of the sample and it also plays the role of potential difference [14]. We will use it to get the moments of $\mathcal{T}$. Taking derivatives with respect to ϕ^2 at zero, details in Appendix B, we get the following linear combinations R_M

$$\begin{aligned}
R_1 = -T_1 &= 2S_1 \\
R_2 = -T_2 + \frac{2}{3}T_1 = S - \frac{G}{3} &= 8S_2 \\
R_3 = -T_3 + T_2 - \frac{2}{15}T_1 &= 32S_3 \qquad (17) \\
R_4 = -45T_4 + 60T_3 - 18T_2 + \frac{4}{7}T_1 &= 5760S_4 \\
R_5 = -315T_5 + 525T_4 - 245T_3 + \frac{85}{3}T_2 - \frac{2}{9}T_1 &= 161280S_5 \\
R_6 = -14175T_6 + 28350T_5 - 17955T_4 + 3840T_3 - 186T_2 + \frac{4}{11}T_1 &= 29030400S_6
\end{aligned}$$

We introduced the sums $S_M = \sum_s s^{-2M}$. The way how to calculate these sums efficiently in any dimension is also in Appendix B. The first two of these equations were derived and the second one compared to numerical simulations in [12] and [13]. The values on rhs are summarized in Table 2.

Recall that for $d \geq 2$ the conductivity $T_1 \to \infty$ and for $d < 2M$ the sums S_M are finite, see Appendix B. One can divide all the equations by T_1 and get a homogeneous system for any C_M. Of course the results are the same as those from Eq. (22). This means, that Nazarov's formula (16) incorporates the

Table 1: Selected values of C_M from Eq. (7). Analytical values of $C_M(1)$ can be deduced from Appendix A

α	C_2	C_3	C_4	C_5	C_6	C_7	C_8
0	$\frac{2}{3}$	$\frac{8}{15}$	$\frac{16}{35}$	$\frac{128}{315}$	$\frac{256}{693}$	$\frac{1024}{3003}$	$\frac{2048}{6435}$
1	0.426217	0.268839	0.196084	0.154259	0.127120	0.108094	0.0940195

diffusive case $\alpha = 0$ of Eq. (7), though the validity of the last goes beyond the mentioned restrictions on dimension (or M). Therefore it is usefull to calculate $1-C_2$ by numerical simulations at 4D and show that the 1/3 suppression holds, see Fig. 3 left. If we would like to derive this analytically also for $d \geq 2M$, the cut-off K could be introduced together with finite sums $S_M(K)$, where the summation is performed only over finite set of $\{n_1, ..., n_d\}$ such that the wave vector length $s < K$. Then we expect $\lim_{K\to\infty} S_M(K)/S_1(K) = 0$ for all $M \geq 2$ and $d \geq 2$.

To proceed with comparing Eq. (16) and the attitude from previous subsection, we would need the ϕ - dependence of the Lyapunov exponents distribution $P(\lambda, \phi)$. We can conjecture that it is independent of λ, i. e. $P(\lambda, \phi) = G(\phi)$, and $G(0) = T_1$. Inserting this into the first expression for the generating function in Eq. (16) and replacing the trace as in Eq. (7), we get:

$$\delta F(\phi) = G(\phi) \int_0^\infty \frac{\cosh(\lambda)^{-2} d\lambda}{1 - \cosh(\lambda)^{-2} \sin^2 \frac{\phi}{2}} = \int_0^\infty \frac{G(\phi)\ d\lambda}{\cosh(\lambda) + \cos\phi} = \frac{\phi}{\sin\phi}\ G(\phi) \tag{18}$$

which is consistent with Eq. (17) at $\phi \to 0$, and comparison to the rhs. of Eq. (16) yields $G(\phi)$. Nazarov [14] introduced yet another quantity $I(\phi) = \phi\ G$ and he gave a formula for the Fano factor in terms of derivatives of I. We are now able to evaluate them:

$$F = \frac{1}{3}\Big(1 - \frac{2\ I'''(0)}{I'(0)}\Big) = \frac{1}{3}\Big(1 - \frac{12\ S_2}{S_1}\Big) \tag{19}$$

We can see again, that the one-third suppression is given by the infinite denominator S_1 rather than by zero numerator (constant, ϕ independent G), as previously assumed.

It also is interesting, that the S_2 value appears in the formula for UCF, e. g. [20], [21]:

$$\langle G^2 \rangle - \langle G \rangle^2 = 12 S_2 = \frac{3}{2}\Big(S - \frac{\langle G \rangle}{3}\Big) = \langle G \rangle - \frac{3}{2} T_2 \tag{20}$$

Table 2: The sums S_M with appropriate factors in dimensions 2, 3 and 4

d	$8\ S_2$	$32\ S_3$	$5760\ S_4$	$161280\ S_5$	$29030400\ S_6$
2	0.123742	0.0387682	0.649759	1.77893	31.9117
3	0.209369	0.0458759	0.699664	1.84186	32.4521
4	∞	0.0573425	0.763394	1.91503	33.0469

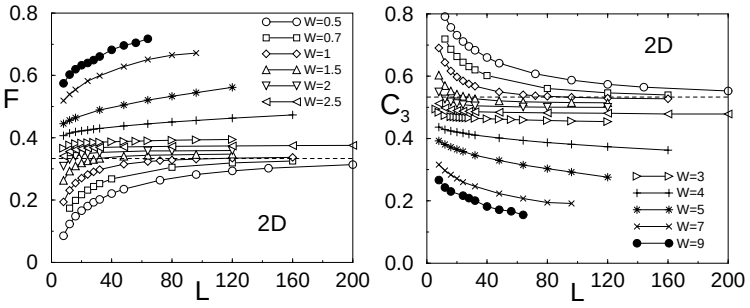

Figure 1: Fano factor $1 - C_2 = F$ and C_3 as a function of system size. The description of disorders applies to both figures. Dashed lines are theoretical diffusive values from Table 1.

3 Numerical simulations

We calculated the mean values of T_M and C_M, $M = 1, 2, ..., 8$ in dimensions $d = 2, 3$ and 4 for various disorders and system lengths L. Typical ensembles were of 10^5 elements for smaller systems and 3×10^4 for the greatest ones.

3.1 Fano factor and C_M

$d = 2$ is lower critical dimension for Anderson model and the case with orthogonal symmetry has still no phase transition. Any positive disorder forces that conductivity tends to zero for very large systems. The obvious inequalities $0 < T_{M+1} < T_M < ... < T_1 = G$ do not mean, that C_M should necessarily tend to zero. Nevertheless this can be expected for extremely large samples, as they approach the localized (Poissonian) regime. From Fig. 1 we see, that C_2, C_3 are monotonic - decaying - functions of L and that the theoretical metallic values are close to the plateau-like region, where the L-dependence is weak. But there is neither any special disorder, nor an asymptotic value, that would be reached. The $C_4, ..., C_8(L)$ dependences look very similarly, just as if they were scaled down to lower values. The $C_M(1/L)$ dependences for $W = 3$ and $M = 2, ..., 8$ in 2D were published already in [9] (and compared to Eq. (22) in [7]), together with 3D data for $W = 10$ and $W_C = 16.5$.

The situation changes substantially in higher dimensions $d > 2$. The metallic limit becomes attractive for disorders $0 < W < W_C$. The MIT is manifested by a constant line at $W = W_C$, which repels neighboring lines on both sides, i. e. also for $W > W_C$, slowly approaching Poissonian limit. This is why we think that any C_M is a good order parameter, the instability of the critical point follows from the scaling hypothesis. In 3D both the metallic and critical values agree very well with theoretical predictions of Eq. (7) for $\alpha = 0$ and 1,

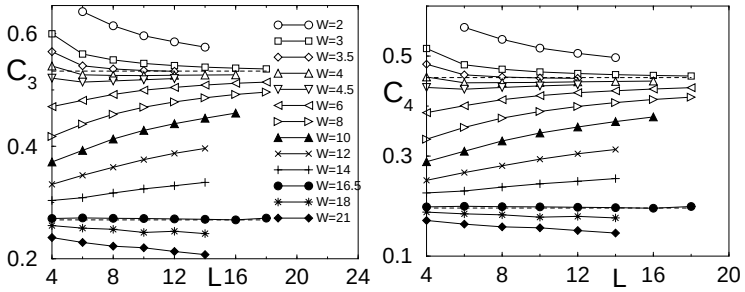

Figure 2: C_3 and C_4 as a function of system size in 3D. The description of disorders applies to both figures. Dashed lines are theoretical values from Table 1.

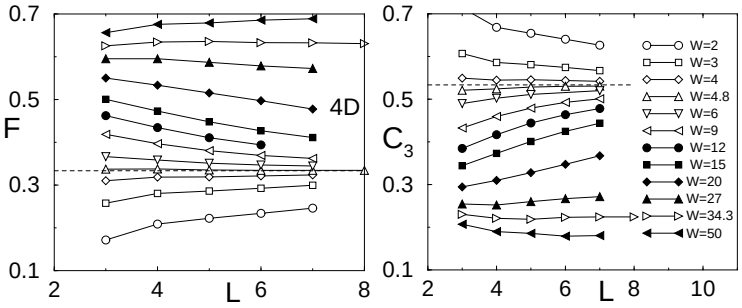

Figure 3: Fano factor $F = 1 - C_2$ and C_3 as a function of system size in 4D. Dashed lines are theoretical metallic values from Table 1. The description of disorders applies to both figures.

respectively, see Fig. 2. Fano factor $F(L)$ has already been published in [13]. Concerning 4D, metallic limits are still the same, as expected, see Fig. 3. But the MIT values are not so easy to understand. We tried several conjectured $P(\lambda)$, e. g. with non-integer α, or a polynomial. None of them could satisfy all C_M values with low number of fitting parameters, though polynomials of the type with $P_C(\lambda) = b_1\lambda + b_2\lambda^2 + b_3\lambda^3$ can fit the moments within several percent. Most probably we have to do with some nontrivial function, too complicated to be found numerically. Not to speak about the possibility of different $P_C(\lambda_1)$. Of course, in 4D we can still have huge finite size effects, spoiling the precision of C_M values at MIT. We leave the 4D $P_C(\lambda)$ question open for future investigations.

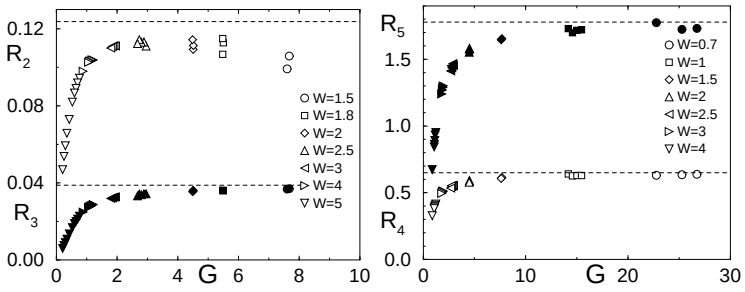

Figure 4: Various R_M quantities as a function of conductivity in 2D. Open symbols are R_2 and R_4, full ones R_3 and R_5. Dashed lines are theoretical values from Table 2.

3.2 Diffusive R_M combinations of T_M

We calculated also the averaged R_M quantities in order to check Eq. (9) numerically. It is usefull to plot them as a function of conductivity G, rather than of L. Fig. 4 left shows, that in 2D the R_2 only roughly approaches the predicted value, at larger G (smaller W) the ballistic regime disturbs the convergence. $R_2(G)$ was shown already in [12]. In order to judge the influence of ballistic, we plot the data also for lower W and L in Fig. 5. Without any disorder ($W = 0$) all $\mathcal{T}_n = 1$ and thus all $T_M = T_1$. So we get the ballistic asymptotics, e. g. $-G/3$ and $-2G/15$ for R_2 and R_3, resp. One can see that the data for low W and L are close to the ballistic asymptotics and with rising L they approach the metallic limit. Surprisingly, for the higher indexed $R_3, R_4, R_5, ...$ this problem becomes less sensitive. Especially if we limit ourselves only to data for the several largest L, their behaviour is almost perfect, Fig. 4, within few percent from theoretical values, Table 2. To overcome the ballistic influence for R_2 fully, we would need even greater L than available.

In 3D there are no signs of disturbing ballistics even for R_2 and our data are in better accordance with predicted value than those in [13]. Again the Eq. (16) is valid without any doubt, see Fig. 6.

The R_2 in 4D is expected to diverge. This is not easy to show numerically, as available system sizes are rather small, Fig. 7 left, and ballistic influence is large again, similarly to 2D. Retrospectively we might even say, that in 2D the R_2 alone was insufficient to confirm any statement. Back in 4D we can just state, that simulated data are in no contradiction with possible logarithmic divergence $R_2 \propto \ln(G) \propto \ln(L)$, which we would expect from analogy with 4D UCF, see [20]. On contrary, $R_3, R_4...$ converge again unexpectedly well to the predicted limits, Fig. 7.

Summarizing, we regard Nazarov's formula (9) as confirmed by numerical

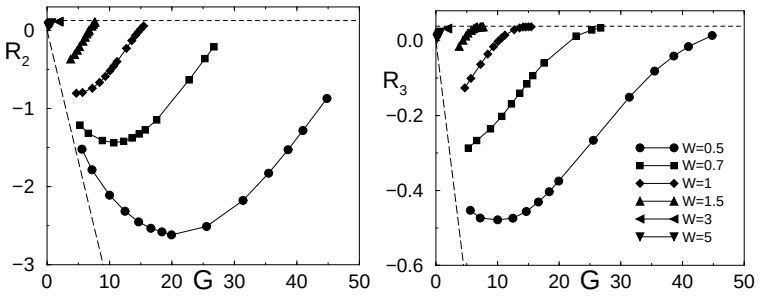

Figure 5: R_2 and R_3 in 2D including smaller W and L. Horizontal dashed lines are metallic theoretical values from Table 2. Long - dashed lines are ballistic limits. The description of disorders applies to both figures.

simulations in Anderson model at least for dimensions up to 4.

4 Conclusions

We have shown all normalized higher current moments C_M can be calculated exactly in the large system size limit at least in next regimes: the diffusive one in virtually any dimension [7], and the critical one (MIT) in 3D. We have confirmed the predicted values by numerical simulations. The MIT in 4D remains an open question. Further we saw, that Nazarov's formula (16) yields the same diffusive C_M values as our Eq. (22) and also special linear combinations of the T_M moments converging to nontrivial constants. We have convincingly confirmed the validity of Eq. (16) for Anderson model in metallic regime by numerical simulations.

5 Appendix A

The aim is to find analytical solution of the integral

$$I_M(\alpha) = \int_0^\infty \frac{x^\alpha}{\cosh^{2M}(x)} dx \tag{21}$$

appearing in the Eq. (5) for $C_M = I_M/I_1$. Special cases known from literature [18] are $\alpha = 0$ (yielding directly the $C_M(0)$ as $I_1(0) = 1$, see [7]):

$$I_M(0) = C_M(0) = 4^{M-1}\mathrm{B}(M,M) = \frac{1}{2}\mathrm{B}(1/2,M) = \frac{\Gamma(1/2)\Gamma(M)}{2\Gamma(M+1/2)} \tag{22}$$

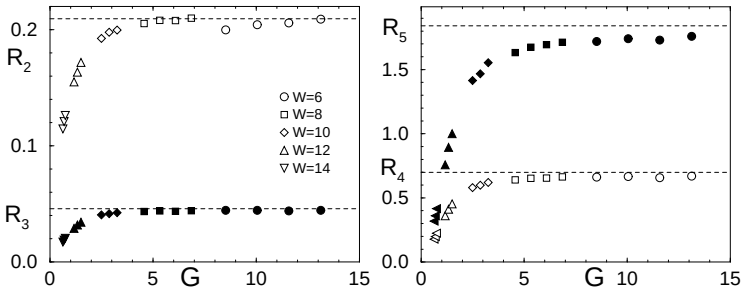

Figure 6: Various R_M quantities as a function of conductivity in 3D. Open symbols are R_2 and R_4, full ones R_3 and R_5. Dashed lines are theoretical values from Table 2. The description of disorders applies to both figures.

and M=1:

$$I_1(\alpha) = 2^{1-\alpha}(1-2^{1-\alpha})\Gamma(\alpha+1)\zeta(\alpha) \quad \text{if } \alpha \neq 1 \tag{23}$$

We introduced the special functions Γ, B and ζ, i. e. the Gamma, Beta and Rieman's Zeta function, respectively, [18]. Further we use the polylogarithmic function $\mathrm{Li}_\alpha(x)$:

$$\mathrm{Li}_\alpha(x) = \sum_{k=1}^{\infty} \frac{x^k}{k^\alpha} \tag{24}$$

more specifically its value at $x = -1$:

$$\mathrm{Li}_\alpha(-1) = -(1-2^{1-\alpha})\zeta(\alpha) \quad \text{if } \alpha \neq 1 \tag{25}$$

$$-\ln 2 \qquad \text{if } \alpha = 1 \tag{26}$$

Without going into details, we found the following exact formulas:

$$I_1(\alpha) = -2^{1-\alpha}\Gamma(\alpha+1)\mathrm{Li}_\alpha(-1) \tag{27}$$

$$I_2(\alpha) = \frac{2^{3-\alpha}}{3!}\Gamma(\alpha+1)[\mathrm{Li}_{\alpha-2}(-1) - \mathrm{Li}_\alpha(-1)] \tag{28}$$

$$I_3(\alpha) = -\frac{2^{5-\alpha}}{5!}\Gamma(\alpha+1)[\mathrm{Li}_{\alpha-4}(-1) - 5\mathrm{Li}_{\alpha-2}(-1) + 4\mathrm{Li}_\alpha(-1)] \tag{29}$$

$$I_4(\alpha) = \frac{2^{7-\alpha}}{7!}\Gamma(\alpha+1)[\mathrm{Li}_{\alpha-6}(-1) - 14\mathrm{Li}_{\alpha-4}(-1) + 49\mathrm{Li}_{\alpha-2}(-1) - 36\mathrm{Li}_\alpha(-1)] \tag{30}$$

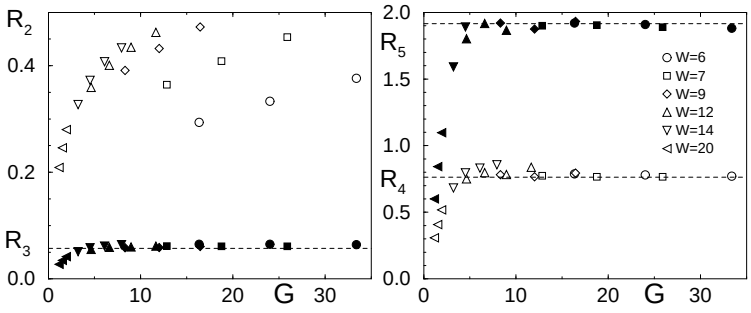

Figure 7: Various R_M quantities as a function of conductivity in 4D. Open symbols are R_2 and R_4, full ones R_3 and R_5. Dashed lines are theoretical values from Table 2. The description of disorders applies to both figures.

$$\begin{aligned} I_5(\alpha) &= -\frac{2^{9-\alpha}}{9!}\Gamma(\alpha+1)[\mathrm{Li}_{\alpha-8}(-1) - 30\mathrm{Li}_{\alpha-6}(-1) + 273\mathrm{Li}_{\alpha-4}(-1) \\ &\quad -820\mathrm{Li}_{\alpha-2}(-1) + 576\mathrm{Li}_{\alpha}(-1)] \qquad (31) \\ I_6(\alpha) &= \frac{2^{11-\alpha}}{11!}\Gamma(\alpha+1)[\mathrm{Li}_{\alpha-10}(-1) - 55\mathrm{Li}_{\alpha-8}(-1) + 1023\mathrm{Li}_{\alpha-6}(-1) \\ &\quad -7645\mathrm{Li}_{\alpha-4}(-1) + 21076\mathrm{Li}_{\alpha-2}(-1) - 14400\mathrm{Li}_{\alpha}(-1)] \qquad (32) \end{aligned}$$

It is worth mention that $\mathrm{Li}_\alpha(-1)$ and $\zeta(\alpha)$ have rational or zero value for α negative integer or zero. In particular, $I_1(1) = \ln 2$, $I_2(1) = -\frac{1}{6} + \frac{2}{3}\ln 2$, $I_3(1) = -\frac{11}{60} + \frac{8}{15}\ln 2$, $I_4(1) = -\frac{19}{105} + \frac{16}{35}\ln 2$, etc. These rationals (the term at $\ln 2$ is $I_M(0)$) can be found much easier with the help of the generator [18]:

$$I_G(t) = \int_0^\infty \frac{x\ dx}{\cosh x + \cos 2t} = 4\frac{t\ln 2 - L(t)}{\sin 2t} \qquad (33)$$

One just takes consecutive odd derivatives at $t = \pi/4$. It is interesting to compare this generator to Eq. (18). Integrating both sides of Eq. (33) w. r. to $y = -\sin^2 t$ yields Eq. (10).

6 Appendix B

In order to get relations for T_M, we will perform n-fold derivation ($n = 0, 1, ..., M-1$) of $\delta F(\phi)$ with respect to ϕ^2 at $\phi = 0$, on both terms from Eq. (16):

$$\begin{aligned} \lim_{\phi\to 0}\delta F &= T_1 = -2S_1 \qquad (34) \\ \lim_{\phi\to 0}\frac{d}{d\phi^2}\delta F = \lim_{\phi\to 0}\frac{1}{2\phi}\frac{d}{d\phi}\delta F &= \frac{T_2}{4} = -2S_2 - \frac{S_1}{3} \qquad (35) \end{aligned}$$

$$\lim_{\phi\to 0}\frac{d^2}{(d\phi^2)^2}\delta F \quad = \quad \frac{1}{24}(3T_3 - T_2) = -4S_3 - \frac{2}{3}S_2 - \frac{7}{90}S_1 \quad (36)$$

etc. We solve this linear system of equations so that we remove almost all the sums S_n, except of the one with the highest index. Thus we get the set of Eq. (17). We choose this one from the plenty of possibilities, because S_M diverges for $d \geq 2M$, like S_2 and R_2 at 4D, Fig. 7. But S_3 is finite at 4D (even 5D) and it can be compared to numerical results. The case $M = 2$ was already treated this way in [12] and [13] and the sums $S_2(d)$ were calculated for $d = 2, 3$.

Now let us show how to calculate the d-fold sums $S_M(d)$ easily with much better precision than by direct summation. The statement is:

$$S_M(d) = \frac{1}{\pi^M 2^d}\int_0^\infty \frac{y^{M-1}}{(M-1)!}[\vartheta_3(0, e^{-\pi y}) - 1][\vartheta_3(0, e^{-\pi y}) + 1]^{d-1}dy \quad (37)$$

Here ϑ_3 is Jacobi elliptic function, simplified to:

$$\vartheta_3(0, q) = \sum_{k=-\infty}^{\infty} q^{k^2} = \frac{1}{\sqrt{y}}\sum_{k=-\infty}^{\infty} \exp\Big(-\frac{k^2\pi}{y}\Big) \quad (38)$$

with $q = \exp(-\pi y)$. The proof of Eq. (37) consists in using the first expansion of elliptic functions and performing per partes $(M-1)$-times. This time the case $M = 2$ was proposed in [20], dealing with universal conductance fluctuations in arbitrary dimension.

Finally let us derive the convergence condition for $S_M(d)$. The values of the expression under integral (37) at small y are crucial. We use the second expansion $\vartheta_3(0, q) \approx 1/\sqrt{y}$ (case $k = 0$) and the leading term is proportional to $y^{M-1-d/2}$. The turning point of convergence is y^{-1}, i. e. $M = d/2$, with logarithmic type of divergence [20].

Acknowledgement

We are grateful to P. Markoš for valuable comments, the VEGA grant Nr. 2/3108/23 for financial support and the Computer Centre of Slovak Acad. Sci. for CPU time.

References

[1] E. Abrahams, P. W. Anderson, D. C. Licciardello, and T. V. Ramakrishnan, Phys. Rav. Lett. **42** 673 (1979)

[2] L. I. Deych, A. A. Lisyansky, and B. L. Altshuler, Phys. Rev. Lett. **84** 2678 (2002)

[3] K. Slevin, P. Markoš, and T. Ohtsuki, Phys. Rev. B **67** 155106 (2003)

[4] K. A. Muttalib, and V. A. Gopar, Phys. Rev. B **66** 115318 (2002)

[5] P. Markoš, K. A. Muttalib, P. Wölfle, and J. R. Klauder, to be published

[6] K. A. Muttalib, J.-L. Pichard, and A. D. Stone, Phys. Rev. Lett. **59** 2475 (1987)

K. A. Muttalib, P. Wölfle, A. Garcia-Martin, and V. A. Gopar, Europhys. Lett. **61** 95 (2003)

K. A. Muttalib, P. Wölfle, and V. A. Gopar, Annals Phys. **308** 156 (2003)

J.-L. Pichard, N. Zanon, Y. Imry, and A. D. Stone, J. Physique **51** 587 (1990)

[7] C. W. J. Beenakker, and M. Büttikker, Phys. Rev. B **46** 1889 (1992)

[8] D. B. Gutman, Y. Gefen, and A. D. Mirlin, in: Quantum Noise in Mesoscopic Physics, ed. by Y. V. Nazarov, Kluwer Acad. Publ., Dordrecht (2003). cond-mat/0210076

[9] J. B. Pendry, A. MacKinnon, and P. J. Roberts, Proc. R. Soc. London A **437**, 67 (1992)

[10] P. D. Kirkman, and J. B. Pendry, J. Phys. C **17**, 5707 (1984)

[11] H. Lee, L. S. Levitov, and A. Yu. Yakovets, Phys. Rev. B **51** 4079 (1995)

[12] A. Kolek, A. W. Stadler, and G. Haldaś, Phys. Rev. B **64**, 075202 (2001)

[13] A. W. Stadler, and A. Kolek, phys. stat. sol. (b) **230**, 267 (2002)

[14] Y. V. Nazarov, Phys. Rev. B **52**, 4720 (1995)

Y. V. Nazarov, Phys. Rev. Lett. **73** 134 (1994)

[15] A. V. Galaktionov, D. S. Golubev, and A. D. Zaikin, Phys. Rev. B **68**, 085317 (2003)

[16] P. Markoš, Ann. Phys. **8**, SI-165 (1999)

[17] P. Markoš, and M. Henneke, J. Phys. - Cond. Mat. **6**, L765 (1994)

[18] I. S. Gradshteyn, and I. M. Ryzhik, Tables of Integrals, Series and Products, Acad. Press, London (1996)

[19] D. Braun, E. Hofstetter, G. Montambaux, and A. MacKinnon, Phys. Rev. B **64**, 155107 (2001)

[20] I. Travěnec, Phys. Rev. B, **69**, 033104 (2004)

[21] P. A. Lee, A. D. Stone, H. Fukuyama, Phys. Rev. B **35** 1039 (1987)